ELSEVIER

A non-parametric electrode model for intracellular recording

R. Brette[a,*], Z. Piwkowska[b], M. Rudolph[b], T. Bal[b], A. Destexhe[b]

[a]*Equipe Odyssée INRIA/ENS/ENPC, Département d'Informatique, Ecole Normale Supérieure, 45 rue d'Ulm, 75230 Paris Cedex 15, France*
[b]*Unité de Neurosciences Intégratives et Computationnelles, CNRS, Bat. 32-33, Avenue de la Terrasse, 91198 Gif-sur-Yvette, France*

Abstract

We present a new way to model the response of an electrode to an injected current. The electrode is represented by an unknown complex linear circuit, characterized by a kernel which we determine by injecting a noisy current. We show both in simulations and experiments that, when applied to a full recording setup (including acquisition board and amplifier), the method captures not only the characteristics of the electrode, but also those of all the devices between the computer and the tip of the electrode, including filters and the capacitance neutralization circuit on the amplifier. Simulations show that the method allows correct predictions of the response of complex electrode models. Finally, we successfully apply the technique to challenging intracellular recording situations in which the voltage across the electrode during injection needs to be subtracted from the recording, in particular conductance injection with the dynamic clamp protocol. We show in numerical simulations and confirm with experiments that the method performs well in cases when both bridge recording and recording in discontinuous mode (DCC) exhibit artefacts. (This work was supported by: CNRS, INRIA, European Commission (FACETS, FP6-2004-IST-FET), Action Concertée Incitative (NIC0005).)

1. Principle

1.1. Modelling the electrode

When recording intracellularly with a single electrode and injecting current at the same time, the recorded potential is

$$V_r = V_m + U_e,$$

where V_m is the membrane potential (which is the variable we are interested in) and U_e is the voltage across the electrode. As a first approximation, the electrode acts as a resistance: $U_e \approx R_e I$, where R_e is the electrode resistance and I is the injected current. Thus a first estimation, known as *bridge compensation*, is $V_m \approx V_r - R_e I$. However, this is too crude an approximation because the electrode has a non-zero charge time and is better modelled by a RC circuit (resistance + capacitance). Amplifiers include a capacitance neutralization circuit which amounts to inserting a negative capacitance in the circuit [8].

Again, this model is too simple because there is always a residual capacitance, which appears as capacitive transients in recorded responses to pulses. These transients can cause serious problems in some situations such as dynamic clamp injection of conductances (injection of current of the form $I(t) = g(t)(E - V_m(t))$ [6,7]), because transients are injected back and can destabilize the system.

Therefore we defined a more complex model of an electrode, by assuming that the electrode can be seen as an arbitrarily complex circuit of resistances and capacitances, which can be represented by a linear time-invariant filter, i.e., the response of the electrode to a current $I(t)$ is expressed as a convolution:

$$U_e(t) = (K_e * I)(t) = \int_0^{+\infty} K_e(s)I(t-s)\,\mathrm{d}s,$$

where $K_e(\cdot)$ is named the *electrode kernel*. The technique consists in identifying the electrode kernel by observing the response of the electrode to a known noisy current. In practice, the electrode kernel can only be estimated when the electrode is impaled into the neuron (because electrode properties change after impalement). In this case, we first

---

*Corresponding author.

E-mail address: brette@di.ens.fr (R. Brette).

remove the membrane kernel from the full measured kernel (see below).

Once the electrode kernel has been estimated, we use the expression above to estimate the voltage across the electrode during injection and subtract it from the recording $V_r(t)$. We named this technique *active electrode compensation* (AEC [2]).

1.2. Intracellular estimation of the electrode model

In the digital domain, the formula reads

$$U_e(n) = \sum_{k=0}^{+\infty} K_e(k) I(n-k).$$

In practice, the electrode kernel K_e vanishes after a short time (a few ms), so that the sum is finite. If $U_e(\cdot)$ is measured and $I(\cdot)$ is known, it is possible to derive the optimal kernel $K_e(\cdot)$ in a least-square sense (in the model, U_e, seen as a vector, depends linearly on K_e). We use sampled white noise as a probe signal $I(n)$ because using a current with minimum autocorrelation enhances the electrode contribution in the recording relatively to the membrane contribution, as the electrode response is at least one order of magnitude faster than the membrane response.

One difficulty in measuring the electrode kernel intracellularly is that we do not observe only the electrode response but also the membrane response. With small white noise, the membrane response is mostly linear, and the recorded potential can be expressed as

$$V_r = V_m + U_e$$
$$= V_0 + K_m * I_e + K_e * I,$$

where K_m is the membrane kernel and I_e is the current actually entering the cell. We assume that I_e is a filtered version of I, with the following expression: $I_e = (K_e / \int K_e) * I$. Thus, we have $V_r = V_0 + K * I$ with

$$K = K_m * \frac{K_e}{\int K_e} + K_e,$$

where K is the full kernel. To extract the electrode kernel K_e, we measure the full kernel K, estimate K_m from fitting an exponential function to the tail of K (this is possible because K_m and K_e have different time scales), and solve the equation above (a direct algorithm follows from expressing the equation with the Z-transform). In fact, fitting an exponential function to the tail of K does not give a correct estimate of the membrane resistance R ($= \int K_m$), which leaves a residual slow exponential tail in our estimation of K_e. The final step in our algorithm is to adjust R so that the tail of K_e is minimized (ideally, it would vanish at the correct value of R). Analytical calculations show that, with this method for estimating the electrode kernel, the relative error in estimating the membrane depolarization (for a constant injected current) of a passive neuron with a simple electrode (resistance +

capacitance) equals the ratio of the time constants τ_e / τ_m, instead of $2\tau_e / \tau_m$ for the simple additive model $K = (R/\tau_m) \exp(-t/\tau_m) + K_e$ (as used e.g. in [1]).

It is important to note that cancellation of the membrane kernel is done only at estimation time, not during subsequent recordings. Therefore changes in membrane properties are not a matter of concern for the method. Changes in electrode properties are, however, a matter of concern, in the same way as with the standard bridge compensation method. To ensure proper operation of the method, the estimation procedure must be run again from time to time. It is not a major inconvenience because the procedure is automatic and fast (a few seconds); besides, our experiments indicate that modifications in electrode properties occur as abrupt changes rather than as a continuous drift in the kernel.

2. Electrode kernels

We measured electrode kernels while recording from cortical neurons in vitro, with a program running in real time (10 kHz) on a computer connected to the amplifier (using a modified version of Neuron [5]). Fig. 1 shows typical electrode kernels, which consists of three phases: first a short period in which the kernel is zero, corresponding to the feedback delay of the system, second a fast rising phase due to acquisition filters, third the electrode decay.

We found that the electrode kernel measured by this method includes, in addition to the characteristics of the electrode per se, all the filters present in the amplifier and the acquisition board, acquisition delays and compensation circuits. Fig. 1A shows electrode kernels measured for various settings of the low-pass filter of the amplifier; Fig. 1B shows kernels for various settings of the capacitance neutralization circuit. At high neutralization level (typical of settings for DCC recordings), one can observe a small damped oscillation (not shown), which is due to the feedback nature of the analogical neutralization circuit in the amplifier. Very close to the onset of unstable oscillations (when there is too much capacitance neutralization), the electrode kernel captures high-frequency oscillations (Fig. 1B, inset).

The method can also be used in the discontinuous current-clamp mode (DCC), which is the standard alternative recording mode when bridge compensation cannot be used [4]: its principle is to alternatively inject and record with a frequency set by the electrode time constant. Ideally, the electrode kernel would be null (the electrode contribution is completely cancelled by the DCC protocol). In practice, the estimation technique often captures a residual kernel which represents the imperfection of the DCC adjustment (Fig. 1C).

We were able to reproduce these effects in numerical simulations. Fig. 1D shows a kernel obtained in simulations of a complex electrode consisting of four resistances and four capacitances; the setup also included
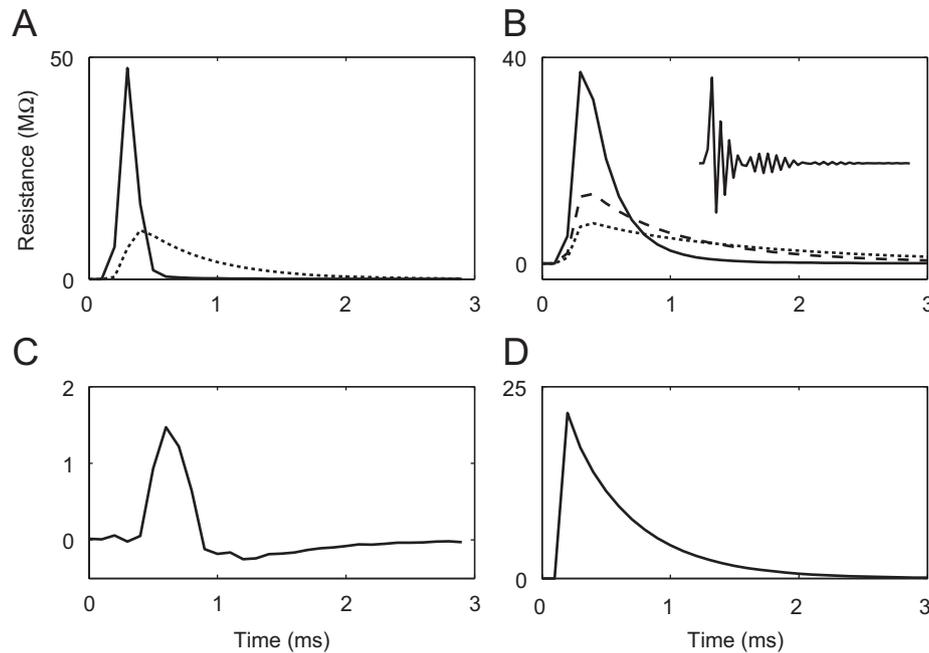
Fig. 1. *Electrode kernels.* (A) Electrode kernel estimated in a cortical neuron in vitro with two settings of the amplifier input low-pass filter: 10 kHz (solid) and 0.3 kHz (dashed). (B) Electrode kernels for three levels of capacitance neutralization (highest level is the solid curve). Inset: electrode kernel close to the "buzz" (maximum level of capacitance neutralization). (C) Kernel of the DCC mode (after adjustment). (D) Electrode kernel of a simulated complex electrode consisting of four resistances and four capacitances ($R_1 = 50\,\text{M}\Omega$, $C_1 = 4\,\text{pF}$, $R_2 = 30\,\text{M}\Omega$, $C_2 = 0.3\,\text{pF}$, $R_3 = 25\,\text{M}\Omega$, $C_3 = 2\,\text{pF}$, $R_4 = 12\,\text{M}\Omega$, $C_4 = 4\,\text{pF}$).

an acquisition delay, which appears as two null steps in the kernel, as in the experiments.

3. Predicting the response of complex electrodes and compensating intracellular recordings

All the results described here were obtained in numerical simulations (in which the true values of electrode parameters and membrane potential are known), then confirmed experimentally in vitro.

3.1. Predicting electrode responses to noisy currents

To show that the method was able to accurately predict the response of an electrode to an injected current, we simulated electrode models consisting of various numbers of resistances and capacitances. The technique allowed us to estimate electrode kernels and predict the response to noisy currents with great accuracy. Fig. 2A shows the response of an electrode consisting of two resistances and two capacitances to white noise current sampled at 10 kHz, together with the estimation using the electrode kernel. The prediction is almost perfect. Then we tested the method when the electrode models were connected to Hodgkin–Huxley-type models of cortical neurons (model and parameters described in [3]). Fig. 2B shows that the electrode kernels extracted by the method differed only slightly from the electrode kernels estimated when the electrodes were isolated. As a result, the response of the

electrode could still be estimated with high accuracy even for fast varying currents (Fig. 2C, response to sampled white noise), except during spikes (arrow in Fig. 2C). Indeed, the method only estimates the voltage across the electrode which results from current injection, but during spikes a large current flows from the neuron through the electrode, and this contribution cannot be estimated. This is not specific to our method, and it would also be obtained when using two electrodes, one for current injection and one for membrane potential recording. The main effect is that spikes are filtered by the electrode (see Fig. 3).

We also simulated more complex recording setups including acquisition delays and more complex electrodes, and found that the method was still able to predict electrode responses in the same way (Fig. 2D).

3.2. Compensating current-clamp recordings

We used these kernels to estimate the voltage across the electrode during current injections and subtract it from recordings in real time, so as to obtain an estimate of the real membrane potential. We refer to this compensation technique as AEC. First, we injected white noise sampled at 10 kHz in a model of a full recording setup (neuron + electrode + amplifier), using AEC to subtract the voltage across the electrode from the recording. The traces showed excellent agreement with the real intracellular membrane potential (Fig. 3A). Note that this is a challenging situation because the electrode voltage to be subtracted is fast and
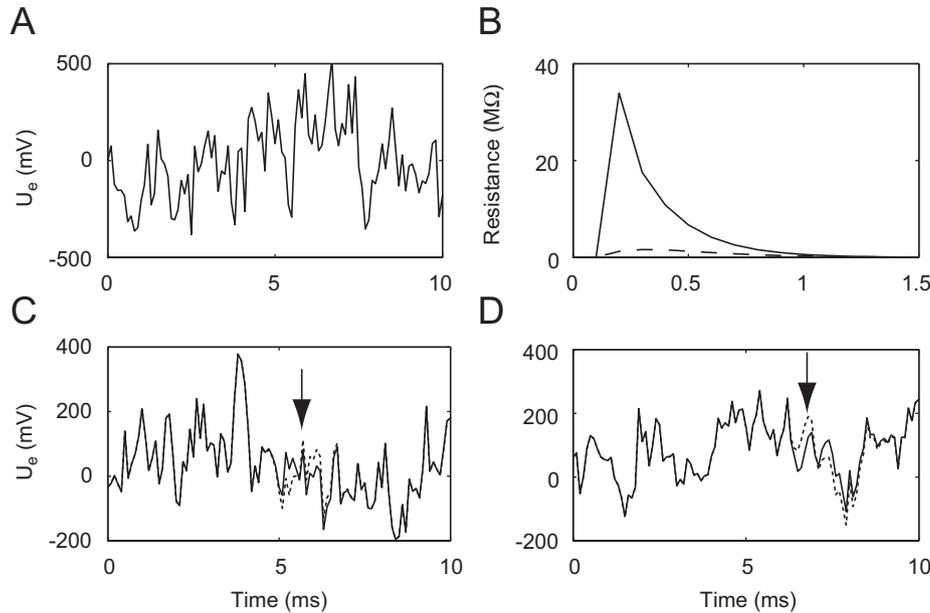
Fig. 2. *Prediction of electrode responses* (*numerical simulations*). (A) Response of an electrode to white noise injection and prediction with the estimated kernel (the curves are perfectly superimposed). The electrode combines two resistances and two capacitances ($R_1 = 50\,\text{M}\Omega$, $C_1 = 2\,\text{pF}$, $R_2 = 30\,\text{M}\Omega$, $C_2 = 1.7\,\text{pF}$). Note the wide scale for electrode voltage U_e. (B) Electrode kernel estimated in bath and after impalement into a neuron are almost identical in simulations (solid curve). The dashed curve shows the difference between the two curves multiplied by 10 (cumulated error is $1\,\text{M}\Omega$). (C) Response of the same electrode to white noise injection when impaled into a neuron (solid) and prediction with the estimated kernel (dashed). Curves are superimposed except during spikes (arrow). (D) Response and prediction for a complex electrode consisting of four resistances and four capacitances (as in Fig. 1D).

can reach $500\,\text{mV}$ (Fig. 2A). Such a noise could not be injected using either bridge compensation (the response contains too many transients) or discontinuous current clamp (the sampling frequency is too low). As noted previously, AEC (as bridge and DCC) cannot correct the filtering of spikes due to current flowing from the neuron through the electrode. Thus spikes appear smaller and wider than they really are (Fig. 3B), and this effect is all the more pronounced that the electrode is slow (Fig. 3C and D). This effect is routinely observed experimentally when recording spikes with different levels of capacitance neutralization. Apart from this effect, AEC correctly compensates the electrode contribution even with complex non-exponential electrodes (Fig. 3C). In extreme situations in which the electrode is very slow (Fig. 3D, note the small spike), AEC is not as satisfying but remains usable (no capacitive transients).

3.3. Compensating dynamic clamp recordings

Then we injected square waves of conductances (in dynamic clamp) in our model (see Fig. 3E). The injected current was a sum of alternating excitatory and inhibitory conductances:

$$I(t) = \alpha H(\sin(2\pi ft))(E_e - V_m(t))$$
$$\qquad + \alpha H(\sin(2\pi ft))(E_i - V_m(t)),$$

where α is the maximum conductance, H is the Heavyside function ($H(u) = 1$ when $u \geqslant 0$, otherwise $H(u) = 0$), f is the

frequency, E_e is the excitatory reversal potential, E_i is the inhibitory reversal potential and $V(t)$ is the membrane potential. Thus, the injected current depends in real time on the measured membrane potential. This is a challenging situation for electrode compensation techniques because errors are amplified by the feedback. In particular, at high frequencies and conductances, simulated bridge recordings were unstable and diverged (growing oscillations), even though they were ideally adjusted, because the residual capacitive transients amplify through the feedback loop of the dynamic clamp. Fig. 3E shows that AEC was able to estimate the membrane potential correctly, while at high frequencies and conductances, DCC recordings had large voltage errors and poor temporal resolution (a model of the DCC was also included in the simulations).

All these numerical results were confirmed experimentally in vitro (see Fig. 3F).

4. Conclusion

The AEC technique, based on a non-parametric linear model of the electrode, allows faithful recordings in continuous mode (and therefore with unlimited sampling frequency) in situations in which bridge compensation cannot be used, including injection of fast currents and conductances. It is also automatic, thus avoiding imprecisions due to subjective manual settings. Future directions include using AEC for in vivo recordings (particularly with sharp electrodes) and for the single-electrode voltage-clamp.
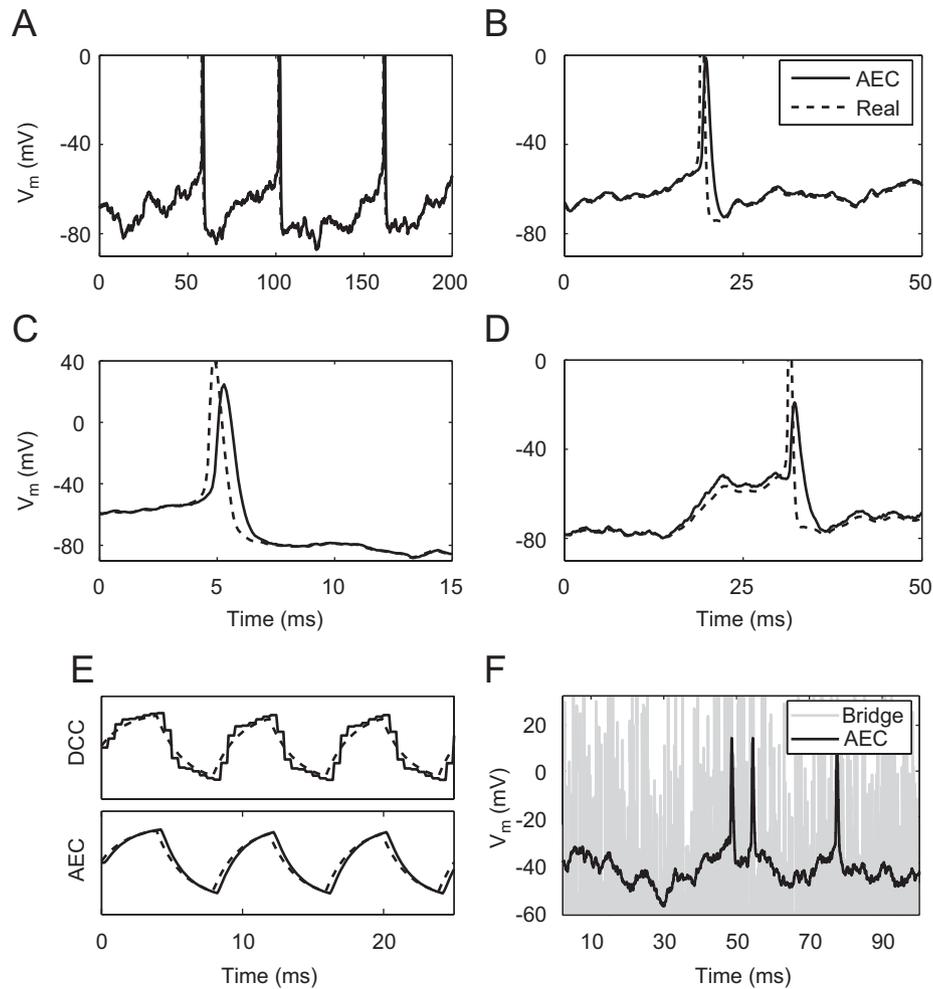
Fig. 3. *Recording with AEC*. (A)–(E) are numerical simulations with a cortical neuron model, F is in vitro. (A) Recording with AEC (solid) vs. real membrane potential (dashed) in the same conditions as for Fig. 2A. (B) Zoom on a spike. (C) Id. with the complex electrode of Fig. 2D. (D) Id. with a very slow electrode ($R_1 = 50\,\text{M}\Omega$, $C_1 = 18\,\text{pF}$, $R_2 = 30\,\text{M}\Omega$, $C_2 = 3.3\,\text{pF}$). (E) Response to a square wave of conductances (solid) vs. ideal response (dashed) for DCC and AEC. (F) Response of a neuron to white noise current recorded with AEC (black) and bridge compensation (grey).

References

[1] J. Anderson, M. Carandini, D. Ferster, Orientation tuning of input conductance, excitation, and inhibition in cat primary visual cortex, J. Neurophysiol. 84 (2) (2000) 909–926.

[2] R. Brette, M. Rudolph, Z. Piwkowska, T. Bal, A. Destexhe, How to emulate double-electrode recordings with a single-electrode? A new method of active electrode compensation (Poster), Soc. Neurosci. Abstracts 31 (2005) 688.2.

[3] A. Destexhe, D. Contreras, M. Steriade, Mechanisms underlying the synchronizing action of corticothalamic feedback through inhibition of thalamic relay cells, J. Neurophysiol. 79 (1998) 999–1016.

[4] A.S. Finkel, S. Redman, Theory and operation of a single microelectrode voltage clamp, J. Neurosci. Methods 11 (2) (1984) 101–127.

[5] M.L. Hines, N.T. Carnevale, The NEURON simulation environment, Neural Comput. 9 (6) (1997) 1179–1209.

[6] A.A. Prinz, L.F. Abbott, E. Marder, The dynamic clamp comes of age, Trends Neurosci. 27 (4) (2004) 218–224.

[7] A.A. Sharp, M.B. O'Neil, L.F. Abbott, E. Marder, The dynamic clamp: artificial conductances in biological neurons, Trends Neurosci. 16 (1993) 389–394.

[8] M.V. Thomas, Microelectrode amplifier with improved method of input-capacitance neutralization, Med. Biol. Eng. Comput. 15 (1977) 450–454.